

Low-ozone pockets observed by EOS-MLS

V. Lynn Harvey,¹ Cora E. Randall,¹ Gloria L. Manney,^{2,3} and Cynthia S. Singleton^{1,4}

Received 18 July 2007; revised 6 March 2008; accepted 21 March 2008; published 5 September 2008.

[1] Earth Observing System (EOS) Microwave Limb Sounder (MLS) observations of ozone are analyzed along with meteorological data from the Met Office using a new automated algorithm to detect low-ozone pockets (LOPs) in stratospheric anticyclones. The algorithm is illustrated with a case study, and all LOPs identified in over 3 years of MLS data are shown. Daily averaged LOP ozone mixing ratios are 5–30% lower than ozone mixing ratios located directly outside a LOP. In the middle stratosphere, near 50° latitude and the Date Line, large LOPs are identified on over 60% of Northern Hemisphere (NH) winter and 50% of Southern Hemisphere (SH) spring days. This suggests that a LOP is present in the Aleutian and Australian anticyclones nearly all the time during these seasons. Ozone reductions in the heart of the LOPs are typically about 20% (10%) in the NH (SH). Thus the LOP contribution to seasonal ozone loss in the anticyclones is estimated at up to ~12% in NH winter and ~5% in SH spring. Average total column ozone loss from individual LOPs is estimated at ~3–6%.

Citation: Harvey, V. L., C. E. Randall, G. L. Manney, and C. S. Singleton (2008), Low-ozone pockets observed by EOS-MLS, *J. Geophys. Res.*, 113, D17112, doi:10.1029/2007JD009181.

1. Introduction

[2] Planetary waves and anticyclones are responsible for much of the large-scale dynamical variability in the winter stratosphere. The effect of planetary waves on long-term ozone trends has been quantified by numerous authors [e.g., Hood *et al.*, 1997, 1999; Fusco and Salby, 1999; Randel *et al.*, 2002; Hadjinicolaou *et al.*, 2002; Hudson *et al.*, 2003, 2006, and references therein]. Using daily Total Ozone Mapping Spectrometer (TOMS) and National Centers for Environmental Prediction (NCEP) data and regression analyses, Hood *et al.* [1999] estimated that up to 40% of the negative midlatitude trend in zonal mean total ozone in February is due to long-term increases in poleward (anticyclonic) wave breaking events in the subtropical lower stratosphere. Randel *et al.* [2002] showed strong positive correlations between total ozone and vertical eddy heat flux at 100 hPa and concluded that wave forcing accounts for ~30% of the trend in midlatitude total ozone. Hood and Soukharev [2005] showed that dynamical influences are responsible for nearly half of the observed negative trend in total ozone at Northern midlatitudes in February and March. Hudson *et al.* [2006] separated total ozone fields into tropical, subtropical, and polar regions based on the position of tropospheric fronts [Hudson *et al.*, 2003]. Their results suggest that the movement of upper tropospheric fronts can

explain 35% of the trend in total ozone. These and other studies [Knudsen *et al.*, 1998; Chipperfield and Jones, 1999; Knudsen and Andersen, 2001; Andersen and Knudsen, 2002, and references therein] provide convincing evidence that dynamical variability is responsible for a significant fraction of ozone variability.

[3] This paper focuses on variations in ozone due to anticyclones, and in particular, low ozone pockets (LOPs) formed therein; this represents a combination of dynamical and chemical influences. In the middle stratosphere, air inside the polar vortices is generally low in ozone, aerosol, and methane and high in water vapor [e.g., Kent *et al.*, 1985; Manney *et al.*, 1994; Lahoz *et al.*, 1994; Randall *et al.*, 1995, 1996; Abrams *et al.*, 1996; Manney *et al.*, 1999; Kreher *et al.*, 1999; Choi *et al.*, 2002]. This is largely a result of air mass separation achieved by the strong polar night jet that encircles the vortex, and subsidence inside the vortex. In general, vortex air is effectively isolated from midlatitudes [e.g., Schoeberl *et al.*, 1992] except during strong stratospheric warming events [e.g., Kleinbohl *et al.*, 2005; Manney *et al.*, 2008b]. Stratospheric warmings occur when planetary waves grow into closed anticyclones that become stronger than the polar vortex.

[4] Like air in the vortex, air in persistent planetary scale anticyclones is also isolated and acquires specific characteristics such as high aerosol [Harvey *et al.*, 1999], filamentary potential vorticity, N₂O, and water vapor surfaces [O'Neill *et al.*, 1994; Sutton *et al.*, 1994; Lahoz *et al.*, 1993, 1994, 1996] and LOPs [Manney *et al.*, 1995; Harvey *et al.*, 2004]. A convincing example of a long-lived anticyclone with distinct chemical properties is the “frozen-in” anticyclone presented by Manney *et al.* [2006]. Manney *et al.* [1995] first observed the formation of a LOP in the Aleutian High using near-global Upper Atmosphere Research Satellite (UARS) Microwave Limb Sounder (MLS) ozone data. LOPs form

¹Laboratory for Atmospheric and Space Physics, University of Colorado, Boulder, Colorado, USA.

²Jet Propulsion Laboratory, California Institute of Technology, Pasadena, California, USA.

³Department of Physics, New Mexico Institute of Mining and Technology, Socorro, New Mexico, USA.

⁴Now at National Science Foundation, Arlington, Virginia, USA.

in the core of high latitude anticyclones because the air is confined to regions where there is less sunlight and thus less production of odd oxygen [Morris *et al.*, 1998; Nair *et al.*, 1998]. This is in contrast to air that encircles the periphery of the anticyclone, which is continuously mixed with lower latitude air and results in ozone mixing ratios that are up to twice as large as in the center of the anticyclone. Manney *et al.* [1995] presented several LOP case studies in each hemisphere, and Harvey *et al.* [2004] documented all LOPs observed by solar occultation (SO) instruments from 1991–2003. However, because the spatial coverage of SO is so poor that many significant LOP events are missed, SO data are insufficient to define a representative climatology of LOPs. Here we use EOS MLS ozone data and meteorological analyses to document LOP frequency of occurrence rates and accompanying ozone reductions, and to provide an estimate of the LOP contribution to midlatitude ozone variability in the middle and upper stratosphere. To accomplish this, an automated LOP identification algorithm is developed to detect LOPs in the EOS MLS data.

[5] Section 2 describes the ozone data and meteorological analyses used in this study. Section 3 presents the new algorithm developed to automate the detection of LOPs. Section 4 illustrates the fidelity of the detection algorithm during a 7-week case study of a LOP that formed in the Arctic winter of 2005–2006. Section 5 presents 3-year seasonal mean MLS LOP frequency of occurrence rates and corresponding ozone reductions. Section 6 briefly discusses the effects of LOPs on column ozone. Conclusions are presented in the final section.

2. Data

2.1. Met Office Data

[6] Global assimilated analyses from the Met Office (MetO) Unified Model are used here to identify the parent stratospheric anticyclones that contain LOPs. Temperature, horizontal wind, and geopotential height products are provided once per day on a 2.5° latitude by 3.75° longitude grid on pressure levels between 1000 hPa and 0.1 hPa [Swinbank and O'Neill, 1994]. The model uses three dimensional variational data assimilation [Lorenc *et al.*, 2000] and has a semi-Lagrangian dynamical core [Davies *et al.*, 2005]. The isobaric data are interpolated to potential temperature surfaces ranging from 330 K (~ 10 km, 150 hPa) to 2000 K (~ 50 km, 1 hPa) where potential vorticity and other diagnostic variables are calculated. One of these diagnostics is a three-dimensional air mass “marker” that is set to -1 for all grid points inside anticyclones, $+1$ for grid points inside the polar vortex, and zero for all other grid points. The algorithm to “mark” the polar vortices and anticyclones involves integrating a strain/rotation parameter within stream function isolopleths (see Harvey *et al.* [2002] for a detailed description of the algorithm). Time series of anticyclone frequency in the upper stratosphere do not show discontinuities in late 2000 or 2003, lending confidence that our results are not sensitive to the changes in the assimilation model. The air mass type corresponding to each MLS measurement is defined by 3D interpolation of the air mass marker field to the MLS measurement location. This “air mass flag” denotes whether each profile is within an anticyclone, within the polar vortex, or in neither (hereafter referred to as “ambient”).

2.2. EOS-MLS Data

[7] The EOS-MLS (hereafter MLS) instrument onboard the Aura satellite was launched in July 2004 [Waters *et al.*, 2006]. In this work we use the version 1.5 data [Froidevaux *et al.*, 2006]. However, after 1 March 2007 only version 2.2 data are available [Froidevaux *et al.*, 2008] and these data are used between March and November 2007. Below ~ 2 hPa, differences between v1.5 and v2.2 stratospheric ozone are on the order of 2% [Froidevaux *et al.*, 2008]. On days when both v1.5 and v2.2 data are available, LOPs identified using the automated algorithm are nearly identical; thus, the results shown here are not sensitive to changing data versions. The estimated single-profile precision for ozone is 0.2 to 0.4 ppmv (2–15%) in the stratosphere [Froidevaux *et al.*, 2008]. Each day MLS retrieves ~ 3400 ozone profiles with near-global coverage. The 3–4 km vertical resolution of the ozone product may limit the ability of MLS to detect LOPs shallower than ~ 6 –8 km. This situation is most common during LOP formation and decay; most LOPs span 10 to 20 km or more [Harvey *et al.*, 2004], however, and these are readily observed. Ozone data are filtered using the status, quality, threshold, and convergence (for v2.2) values provided by the MLS science team [Livesey *et al.*, 2008; Froidevaux *et al.*, 2008].

3. Low-Ozone Pocket Definition

[8] Harvey *et al.* [2004] defined LOPs in SO data from visual inspection of the data. This is impractical for MLS, which has two orders of magnitude more data than the SO instruments on a daily basis; thus an automated algorithm to detect LOPs in the MLS data was developed. The largest (both spatially and with the lowest ozone) Arctic LOP since the beginning of the MLS data record is used here to illustrate the LOP detection algorithm; it also emphasizes how drastically LOPs can alter global ozone distributions. In section 4, results using the algorithm will be shown for more moderate LOPs during a 7-week case study of this event.

[9] The automated LOP detection algorithm takes advantage of the dense MLS observation coverage. To identify LOPs on each day, the distribution of ozone inside an anticyclone is compared to ambient ozone nearby but outside the anticyclone. Comparisons are made as a function of altitude in each hemisphere. “Nearby” is defined relative to the center of mass of the anticyclone. A circular region centered on the anticyclone center of mass at each altitude is defined with a radius equal to 500 km plus the distance from the center to the furthest edge point of the anticyclone. The area between the edge of the anticyclone and this circle is the region of “ambient” ozone. The following additional logic is added to improve the performance of the LOP algorithm. (1) If the circular region extends equatorward of 20° latitude, it is truncated at 20° so as not to include high tropical ozone data that would elevate ambient ozone and result in false positive LOP identification. (2) If the circular region extends into the polar vortex, these data are excluded to avoid including low ozone that would obscure LOPs that do exist.

[10] To define the LOP at each altitude nearby ambient ozone is compared to ozone inside the anticyclone itself. Mean and standard deviation profiles are calculated for

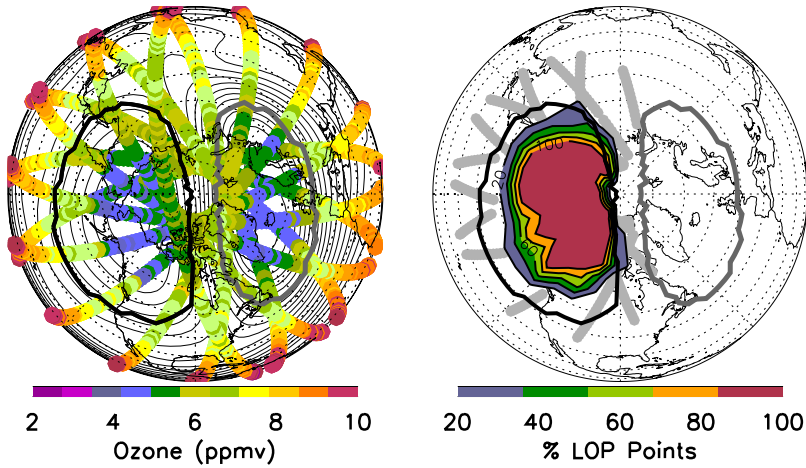


Figure 1. NH polar orthographic projections at 1000 K on 12 January 2006 with the Greenwich meridian oriented to the right. The left panel shows MLS ozone (color), the edge of the Arctic vortex (thick, grey) and Aleutian High (thick, black), and the stream function field (thin, black contours). The right panel shows the edges of the Arctic vortex and Aleutian High as in the left panel. Superimposed are ambient data points (grey) identified at this level (see text for details). The % of all MLS data points identified as LOP points, binned every 10° latitude and 15° longitude, is color contoured.

ozone data located inside the anticyclone as well as in nearby ambient regions. Individual LOP data points are defined as ozone values in the anticyclone that fall below mean nearby ambient ozone minus 1 standard deviation in ambient ozone. Between ~ 700 K and ~ 1500 K (~ 25 – 40 km), large horizontal gradients in ozone are common and LOPs are easy to identify both visually and using the automated detection algorithm. Above and below these altitudes, the standard deviation in ambient ozone is small and some false positive LOP identifications occur. In order to minimize this effect we require at least 50 LOP data points to be flagged on each day. In general, only one LOP is identified in each hemisphere on each altitude and day. On less than 5% of the days; however, during anticyclone merger events, there are two anticyclones very close to each other and there remain ambiguities in the determination of LOPs on these days.

[11] Figure 1 illustrates the detection algorithm with the most extreme LOP observed in the MLS data set. Thus this figure portrays data from the NH at 1000 K (~ 33 km) on 12 January 2006, when this LOP was near its peak intensity. MLS ozone mixing ratios (left panel) are significantly lower in both the vortex and anticyclone than in the surrounding air. In the right panel, MLS measurements within the circular region but outside the anticyclone are defined as nearby ambient data points (grey symbols). Since the anticyclone is smaller above this altitude, and since MetO air mass information is interpolated to this level in three-dimensions (not just horizontally) an artifact of the definition is that some ambient data points intersect the edge of the anticyclone. The fraction (%) of MLS measurements identified as LOP points at this altitude is expressed by the color contours; note that these contours are clustered in the core of the anticyclone. Latitude-altitude and longitude-altitude sections through the LOP indicate a poleward and westward tilt of with altitude (not shown) following the shape of the anticyclone on this day.

[12] Figure 2 shows daily mean ozone profiles \pm one standard deviation in the Aleutian High (red), in nearby ambient regions (black), and in the LOP (blue) on 12 January 2006. Mean LOP ozone is 15–23% lower than ambient ozone between 700 K and 1800 K (~ 25 – 45 km). Single profile differences at each altitude often exceed 50% (not shown). Because the LOP is defined as anticyclone ozone that is 1 sigma lower than mean ambient ozone, at all altitudes there are a small number of ambient points with ozone values lower than the LOP threshold value that are not flagged as LOP points. Above 1800 K and below 700 K where ozone mixing ratios are small everywhere, identifi-

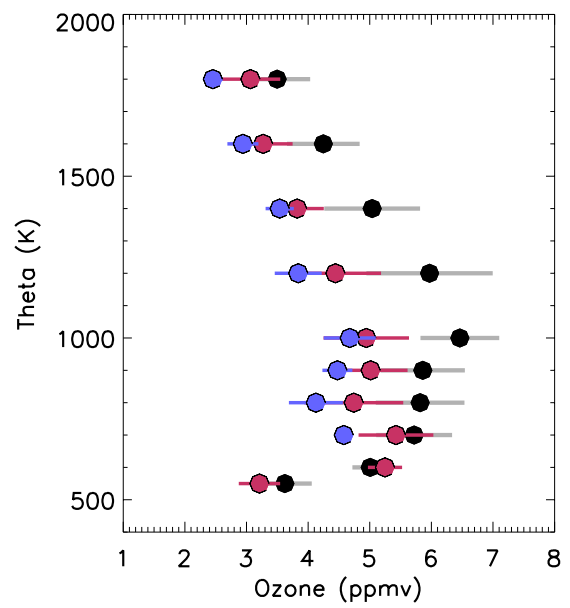


Figure 2. Daily mean MLS ozone profiles \pm one standard deviation in the Aleutian High (red), in nearby ambient regions (black), and in the LOP (blue) on 12 January 2006.

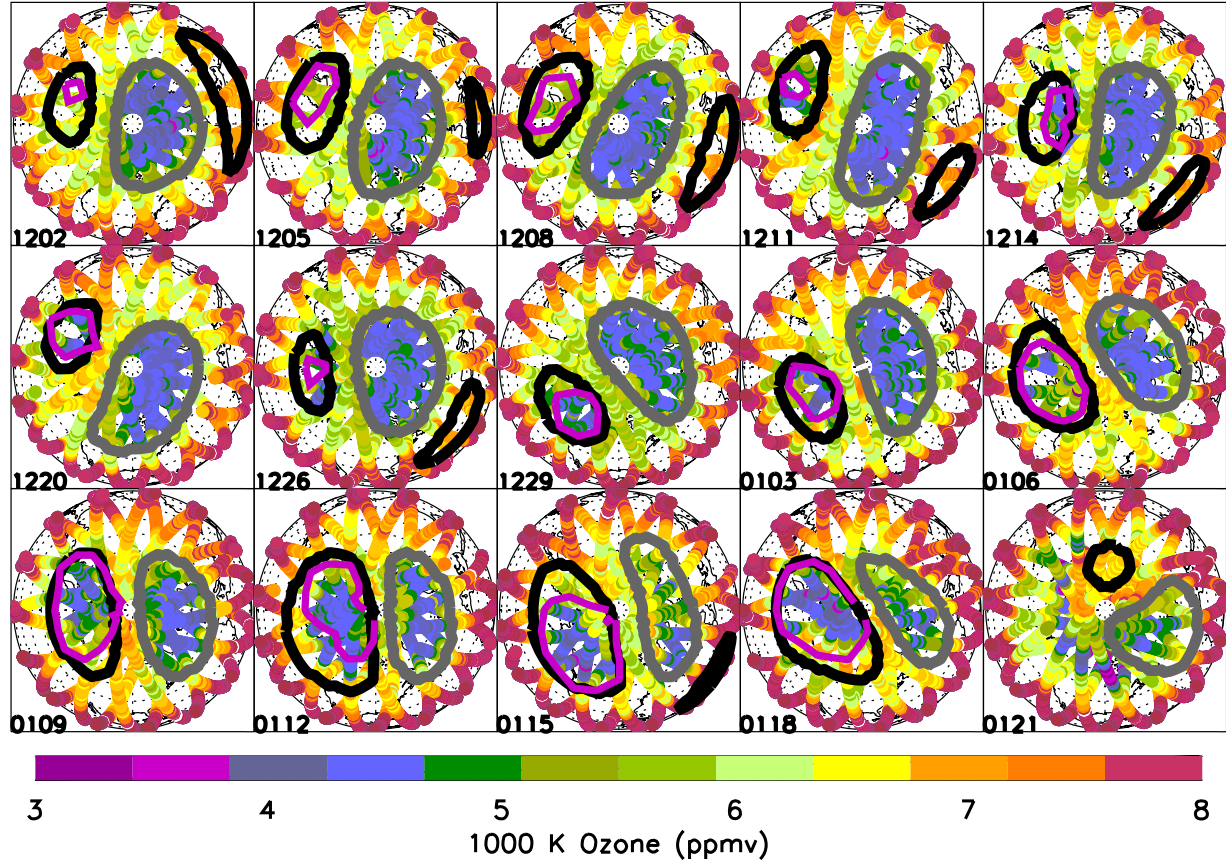


Figure 3. NH polar orthographic projections of MLS ozone (in color), the Arctic vortex (grey contour), and anticyclones (black contours) at 1000 K. The Greenwich meridian is oriented to the right. Every third day is shown between 2 December 2005 and 21 January 2006. The pink contour inside the Aleutian High (near 50°N latitude and the Date Line) represents where more than 50% of MLS data points, binned every 10° latitude and 15° longitude, are LOP points.

cation of LOPs is more difficult and some false positives occur. Overall, results are not sensitive to the magnitude of the ozone threshold set by the 1-sigma criterion. Occurrence frequency and general characteristics remain unchanged when using threshold values of 1.25 and 1.75 sigma (not shown).

4. Low-Ozone Pocket Case Study 2005–2006

[13] The LOP described above persisted with varying intensity for 7 weeks. In this section we describe in more detail the evolution of this LOP. The analysis here illustrates the fidelity of the LOP detection algorithm on days in December 2005 when the LOP is more moderate in size and ozone content. This event is described here from several different perspectives.

4.1. Polar Perspective

[14] Figure 3 shows NH polar orthographic projections of MLS ozone (in color), the Arctic vortex (thick grey contour) and anticyclones (thick black contours), and the % frequency of MLS measurements identified as LOP points (pink contour) at 1000 K (~33 km; near the middle of the LOP) every third day between 2 December 2005 and

21 January 2006. The Aleutian High formed on about 22 November and moved east and west about the Date Line during December and January. Polar perspectives such as these clearly show ozone gradients aligned with the vortex and anticyclone boundaries. LOP points are identified in the Aleutian High on every day shown here, including days in early December when the LOP is weak. This figure summarizes the horizontal extent and movement of the LOP at this altitude over its 7-week lifetime.

[15] The Aleutian High slowly moved eastward in December and strengthened. In January this anticyclone is larger than the vortex throughout the stratosphere and contains ozone as low as that in the vortex. Maximum % frequency of MLS measurements identified as LOP points consistently reaches 100% in regions inside the Aleutian High. This extremely strong anticyclone is associated with a major sudden stratospheric warming event that began on 20 January and lasted for nearly a month in the lower stratosphere [Manney et al., 2008a]. By 21 January, the Aleutian High dissipates at this altitude and low ozone from the LOP and from the vortex mix together. Meanwhile, another very strong anticyclone moves rapidly from low latitudes toward the pole; ozone within the core of this “young” anticyclone has not yet decreased to the lower

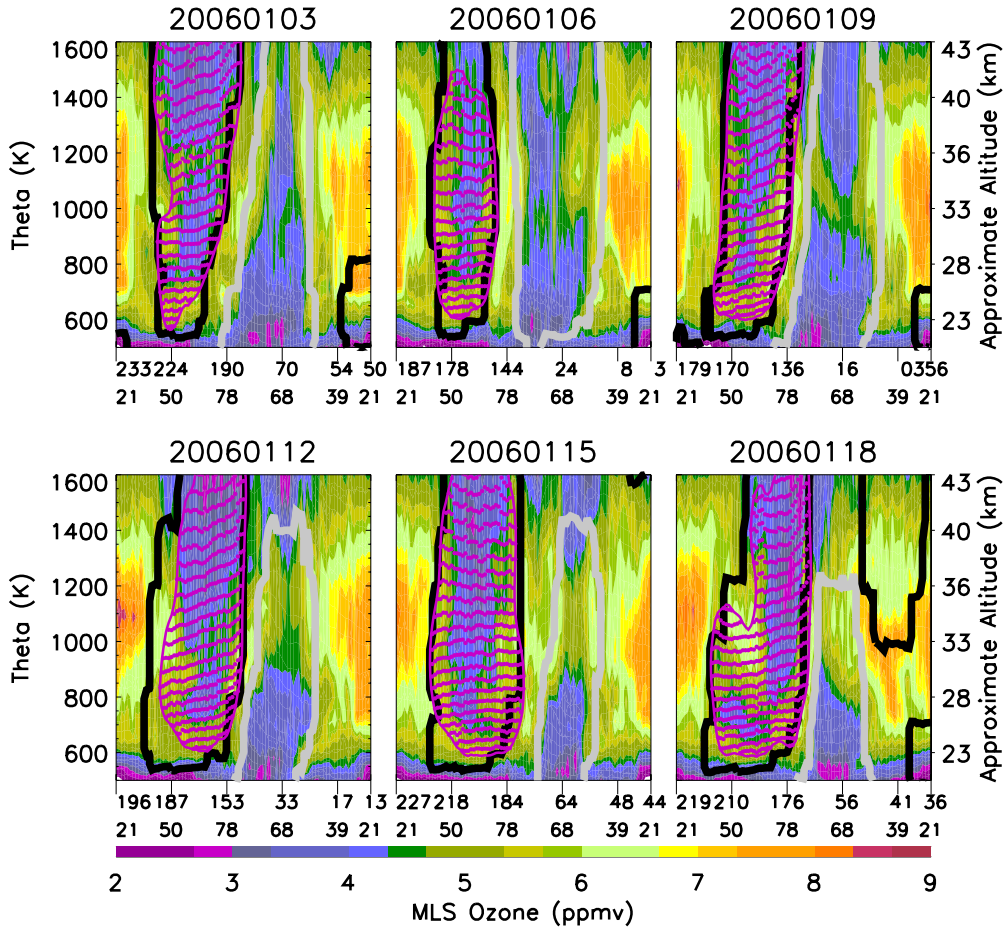


Figure 4. Cross-polar vertical sections of MLS ozone mixing ratio (in color) that intersect the Arctic vortex (thick, light grey) and anticyclones (thick, black) on 3, 6, 9, 12, 15, and 18 January 2006. Individual LOP points are superimposed (pink symbols). The range of potential temperature (altitude) surfaces is shown on the left (right). Longitudes and latitudes of each section are given along the x axis.

equilibrium ozone value associated with high latitudes, however, and thus does not contain a LOP.

4.2. Cross-Polar Ozone Perspective

[16] Figure 4 illustrates the vertical extent of the LOP using cross-polar vertical swaths of MLS ozone mixing ratio (color). This is a useful way to view LOPs since they are vertically deep features ($\sim 10\text{--}20$ km) and multiple levels can be observed simultaneously. MLS orbits are chosen that intersect the Arctic vortex (grey contour) and anticyclones (black contours) on 6 days between 3 January and 18 January 2006. Individual MLS data points that have been identified as LOP points are superimposed (pink symbols).

[17] At each altitude, ozone gradients are large near the edge of vortex and anticyclone. On 3 January, the LOP extends from $\sim 35\text{--}45$ km and spans $\sim 40^\circ$ of latitude wherein ozone is reduced by 2 ppmv ($\sim 30\%$). The spatial extent of the LOP covers thousands of square kilometers over the North Pacific. Higher ozone is located directly outside the LOP (between the anticyclone and the vortex, below the LOP, and in the Tropics). Over the next week, the LOP expands both horizontally and vertically. By 12 January, the anticyclone is larger than the vortex and ozone in the LOP is lower than ozone in the vortex from

$\sim 30\text{--}40$ km. Over the next 6 days, the LOP persists and the vortex weakens. On 18 January, the Aleutian anticyclone and LOP tilt poleward and a second anticyclone is observed above ~ 33 km near 40°N latitude and 40°E longitude. Ozone mixing ratios in the second anticyclone are depleted near 35 km; however, a LOP is not identified. Within a day or two, the Aleutian High and the LOP rapidly dissipate at all altitudes (not shown) and the second anticyclone moves over the pole.

4.3. Time-Altitude Perspective

[18] Figure 5 shows the altitude-time evolution of ozone within the Aleutian High (top), nearby ambient regions (middle) and the percent difference between the two (bottom) from 15 November 2005 to 15 February 2006. This analysis is similar to Plate 6 by Manney *et al.* [1995]. Black dashed lines in the top panel indicate approximate dates that traveling anticyclones merged with the Aleutian High above ~ 40 km. Anticyclone merger events are known to strengthen the Aleutian High and weaken the polar vortex [e.g., Scott and Dritschel, 2006]. While anticyclone ozone continually decreases between 25 and 43 km, the last four anticyclone merger events coincide with brief increases in ozone mixing ratios followed by rapid decreases. For the

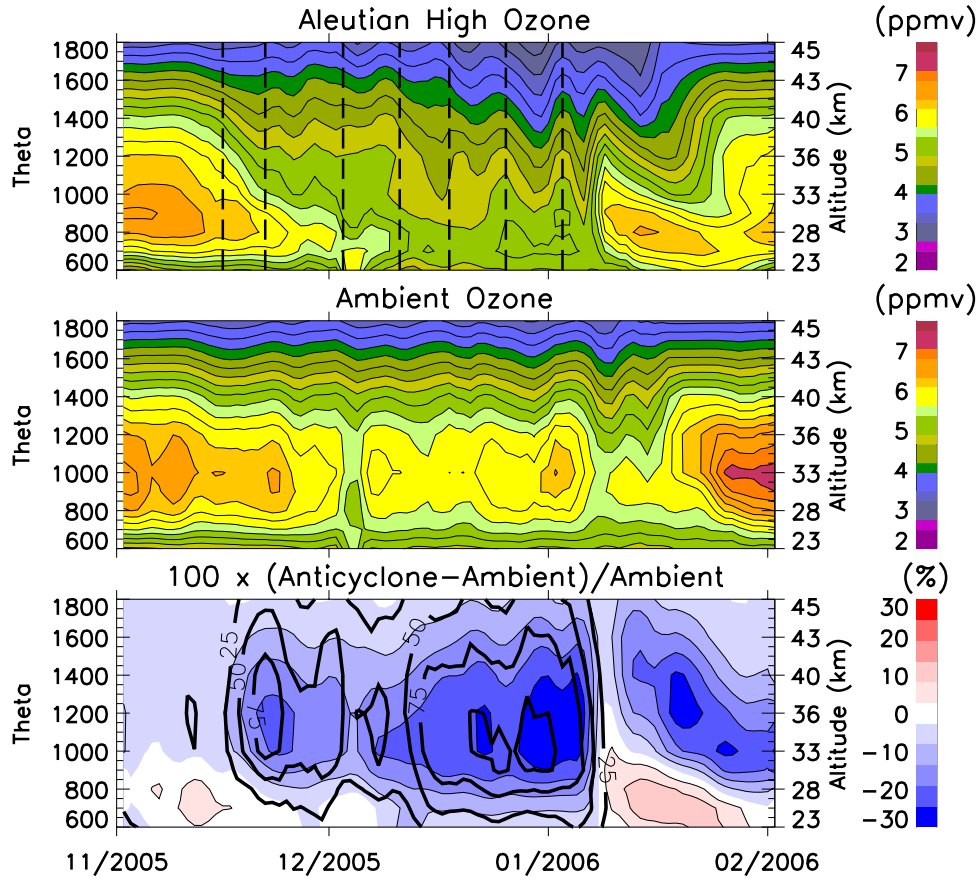


Figure 5. Altitude-time series of MLS ozone from 600 K to 1600 K in the vertical and from 15 November 2005 through 15 February 2006. Date labels are on the 15th of each month. The top panel shows daily mean ozone inside the Aleutian High. Black dashed lines indicate approximate dates of anticyclone merger events. The middle panel shows daily mean ozone in nearby ambient regions. The bottom panel shows the percent difference between the two (in color). Superimposed is the % of MLS data points in the Aleutian High that are identified as LOP points on each day and altitude (black contours).

most part, LOPs only form in the Aleutian and Australian anticyclones and are not observed in the traveling anticyclones. This is because traveling anticyclones are generally not as persistent as the quasi-stationary anticyclones and they are observed at lower latitudes. However, a day or two prior to an anticyclone merger event (when the traveling anticyclone moves poleward), LOP points are sometimes identified in the traveling anticyclone above 35 km (not shown). An analysis of the modulation of LOPs during anticyclone merger events is beyond the scope of this paper and is the subject of future work.

[19] Black contours in the bottom panel represent the % of MLS data points in the Aleutian High that are identified as LOP points. In late-November 2005, LOP points are first detected at 1200 K (~ 36 km). Following the first anticyclone merger event in early December 25% of MLS data points are identified as LOP points between ~ 25 and 45 km. This is consistent with the Aleutian High strengthening and continuing to effectively confine air within it. Over the next 7 weeks ozone in the LOP decreases at all levels and the number of LOP points identified increases. By early January daily mean ozone in the Aleutian High is 30% lower than daily mean ambient ozone between 1000 K and

1400 K, and over 75% of MLS data points in the anticyclone are flagged as LOP points. As the ozone differences become more negative, more LOP points are identified. This gives confidence that the LOP detection algorithm is reliable. The number of LOP points decreases both above ~ 40 km and below ~ 30 km because the mechanism by which LOPs form depends critically on the chemical and dynamical timescales for ozone being comparable. In the upper (lower) stratosphere the chemical timescales for ozone are too short (long). On 21 January 2006, the Aleutian High and the LOP dissipate as the vortex breaks down during the major stratospheric warming event. Less than 5% of MLS data are identified as LOP points in the anticyclone that formed in early February.

5. Three Years of MLS LOP Observations

5.1. Seasonal Zonal Means

[20] Figure 6 shows seasonal zonal mean ozone differences (%) between LOPs and ambient air (in color) and zonal mean LOP frequency of occurrence (%, black contours) between September 2004 and November 2007. In the

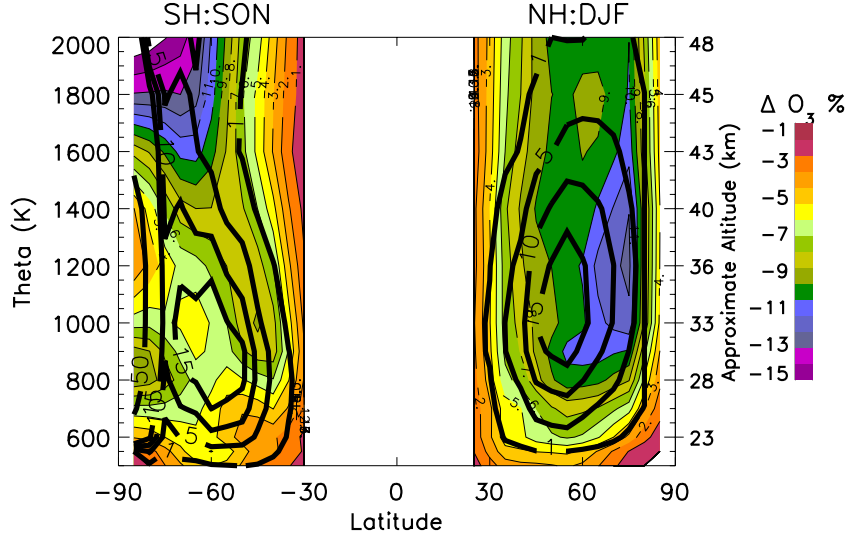


Figure 6. Three-year seasonal zonal mean ozone difference (%) between LOPs and ambient air (in color) and zonal mean LOP % frequency of occurrence (black contours) between September 2004 and November 2007. In the NH (SH), statistics are calculated from the months of December, January, and February (September, October, and November). MLS data are binned every 5° latitude on potential temperature surfaces ranging from 500 K to 2000 K.

NH (SH), statistics are calculated from the months of December, January, and February (September, October, and November); these months are used because they coincide with the highest frequency of anticyclone occurrence

[e.g., Lahoz *et al.*, 1996; Harvey *et al.*, 2002]. Thus NH (SH) LOPs that form in November and March (August) are not included in this analysis. Recall that we require more than 50 LOP data points per day over the altitude range to

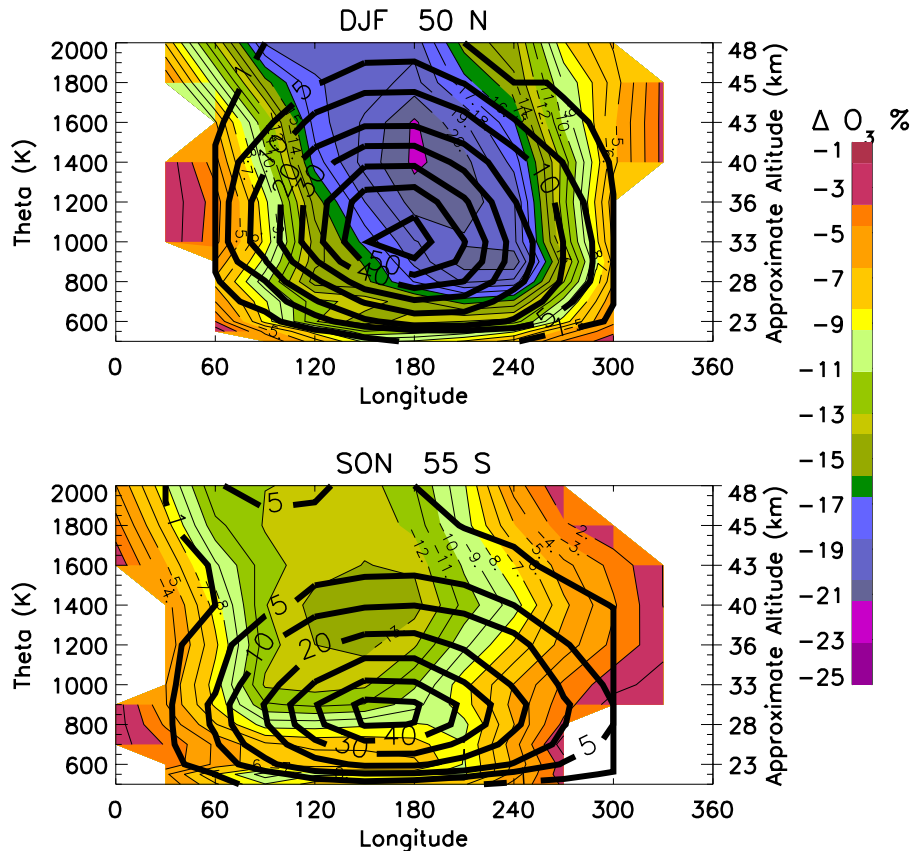


Figure 7. Three-year seasonal longitude-altitude sections as Figure 6 at 50° N (top) and 55° S (bottom) latitude. MLS data are binned every 30° longitude.

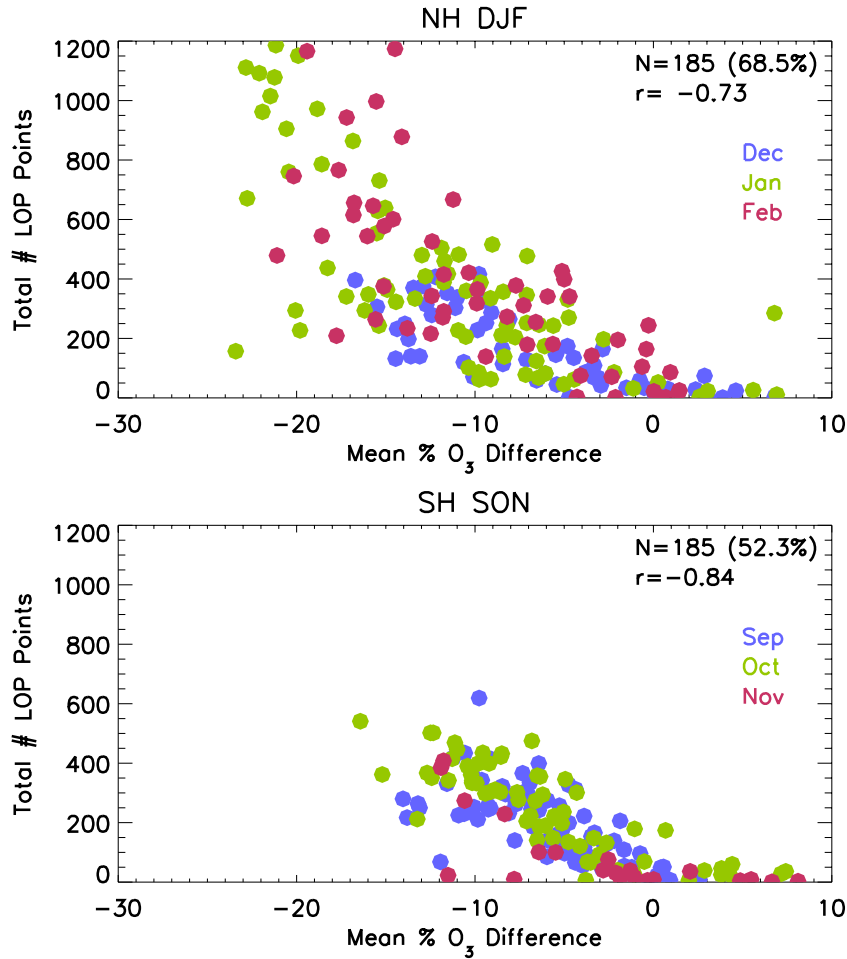


Figure 8. Scatterplots of daily mean % ozone differences between LOPs and ambient air (x axis) versus the total number of daily LOP points (y axis) during 3 NH winter (top) and 4 SH spring seasons (bottom). Daily mean ozone differences and total LOP points are computed using all data in the 800 K to 1400 K ($\sim 28\text{--}40$ km) vertical layer. Points are colored by month, N equals the number of data points, in parentheses is the % that N is of all days considered, and r is the correlation coefficient.

minimize the effects of including very small or false positive LOPs. At the LOP frequency maxima (between 800 K and 1200 K and 50°–70° latitude in both hemispheres) LOP points comprise over 15% of all MLS data points during the NH winter and SH spring seasons. Near these two LOP frequency maxima, seasonal zonal mean ozone is 10% (5%) lower in LOPs than ambient air in the NH (SH). Thus if the behavior in 2004–2007 is representative, from 50°–70° latitude and from $\sim 28\text{--}36$ km LOPs reduce zonal mean seasonal ozone by about 1.5% (0.75%) in the NH (SH).

[21] While LOPs exhibit many similar characteristics in the Arctic and Antarctic, notable differences include the following. In the SH, as anticyclones move progressively closer to the pole in the spring, more LOP points are identified at high southern latitudes. The LOP frequency maximum near the South Pole occurs during the Antarctic final warming when the summer anticyclone forms over the pole. In the NH, the LOP frequency maximum does not extend to the pole because LOP points are identified most often inside the wintertime Aleutian High typically located near 55°N [Harvey and Hitchman, 1996]. The % frequency

of occurrence field suggests that SH midlatitude LOPs form at lower altitudes than those in the NH. This hemispheric difference is attributed primarily to the timing of SH anticyclones (and LOPs) in that they occur in spring when ozone production becomes significant, resulting in shallower LOPs. The anticyclones during southern spring are also more mobile [Mechoso *et al.*, 1988; Manney *et al.*, 1991; Lahoz *et al.*, 1996] and this may inhibit deep LOP growth.

5.2. Seasonal Means as a Function of Longitude

[22] Figure 7 shows 3-year seasonal longitude-altitude sections of ozone differences (%) and LOP frequency of occurrences at 50°N (top) and 55°S (bottom) latitude. These latitudes intersect the two midlatitude zonal mean LOP frequency maxima shown in Figure 6. It is well known that the longitude sector over the Pacific is a preferred location for mature, high-latitude stratospheric anticyclones that form in Northern winter and Southern spring [Mechoso *et al.*, 1988; Lahoz *et al.*, 1996; Harvey *et al.*, 2002 and references therein]; and it is in these persistent anticyclones that nearly all LOPs are observed. In both hemispheres,

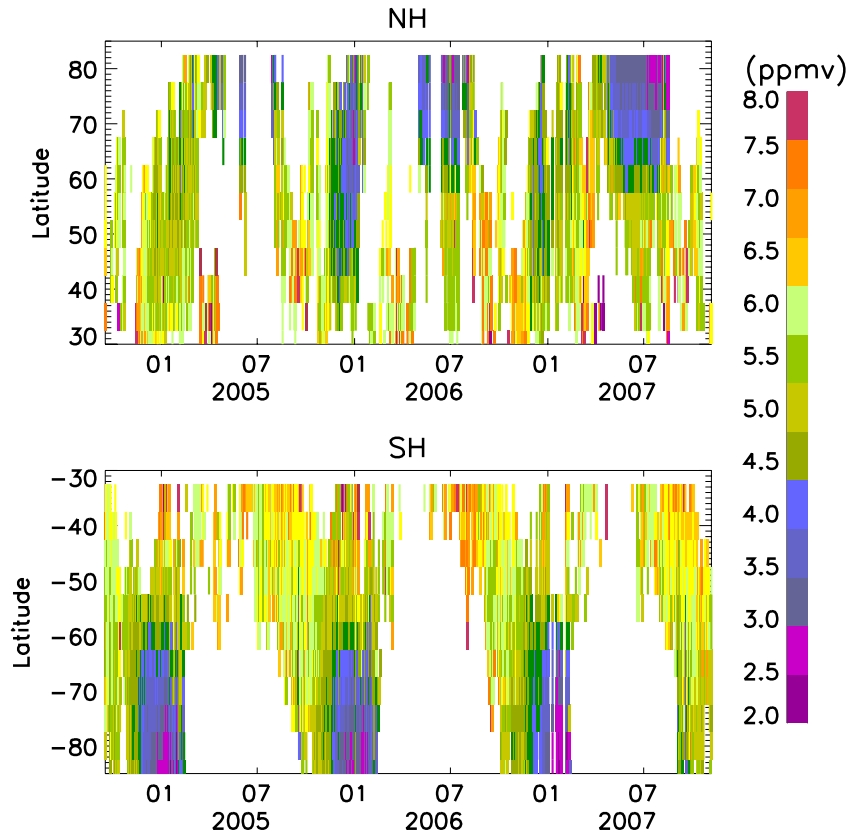


Figure 9. Latitude-time sections of minimum LOP ozone between September 2004 and November 2007 in the NH (top) and SH (bottom). Daily minimum LOP ozone is computed from LOP data points in the 600 K to 1600 K vertical layer binned every 2.5° latitude.

95% of LOPs are identified within 120° longitude of the Date Line; they were never detected within 20° of the Greenwich meridian. In the NH, near the Date Line and 1100 K (~ 32 km), over 60% of MLS data points are identified as in LOPs. Harvey and Hitchman [1996] found that the Aleutian High is present at this location over 60% of the time during Northern winter. These results suggest that a LOP is present inside the Aleutian High nearly all the time. Ozone is reduced by $\sim 20\%$ at this LOP frequency maximum. In the SH, near the Date Line and 800 K (~ 28 km), over 50% of MLS measurements are in LOPs and ozone is reduced by $\sim 10\%$. Thus in regions where LOPs frequently occur, seasonally averaged estimates of the LOP contribution to ozone variability are 12% in the NH and 5% in the SH. Since LOP frequency of occurrence rates are longitudinally dependent, these estimates are significantly larger than the zonal means. Above 1800 K and below 600 K, LOP frequency of occurrence rates are less than 5%. The magnitude of the ozone differences presented here agrees with monthly mean results of Harvey *et al.* [2004] based on SO data. While SO instruments correctly measure the average effect of LOPs, they do not observe many individual LOP events. Therefore future work will explore whether SO instruments capture the same amount of ozone variability in stratospheric anticyclones as observed by MLS.

[23] Figures 6 and 7 showed LOP ozone reductions averaged over many individual LOP events. Figure 8 shows

scatterplots of daily mean ozone differences due to LOPs versus the total number of daily LOP points during three NH winter and four SH spring seasons. As expected, more LOP points are detected as ozone differences increase in magnitude; maximum differences reach 23% (16%) in the NH (SH). In the NH (SH) during January and February (September and October), ozone differences are larger and more LOP points are identified than in other months; this is a direct consequence of increased anticyclone strength and longevity. On days in which fewer than 50 LOP points are detected, mean ozone differences are primarily negative but can also be positive. These points are associated with “false positive” LOP identification or occur on days when a LOP is shallow and does not extend over the full vertical range being averaged.

[24] Thus far, LOP statistics have been restricted to NH (SH) winter (spring) seasons. Figure 9 shows the minimum ozone as a function of time and latitude in all MLS LOPs detected between September 2004 and November 2007. In both hemispheres, LOPs are first identified near 30° latitude and move poleward over their lifetimes. Minimum LOP ozone decreases from fall to spring as LOPs move progressively poleward. This is because the chemical equilibrium value for ozone is lower at higher latitudes, and LOPs at higher latitudes have had more time to approach that value. LOPs are identified over the pole in the summer anticyclone

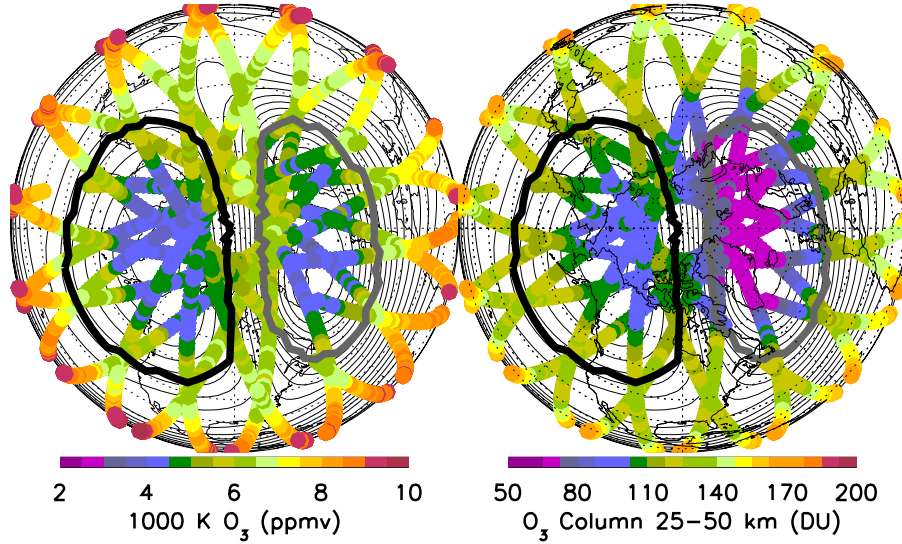


Figure 10. NH polar orthographic projections on 12 January 2006 of MLS ozone mixing ratio at 1000 K (left) and MLS partial column ozone (right). The Greenwich meridian is oriented to the right. The black (grey) contour indicates the edge of the Aleutian High (Arctic vortex) at 1000 K (~ 35 km).

in both hemispheres; however, ozone variability in the summer anticyclone will be the subject of future work.

6. Effect of LOPs on the Ozone Column

[25] It is of interest to quantify the amount that the ozone column is reduced due to the presence of a LOP. The effect of the LOP on 12 January 2006 is shown here as an example. Note that this is the most extreme LOP in the MLS data record, so typical effects are smaller. Figure 10 shows MLS ozone mixing ratios at an altitude central to the LOP (left panel). On this day, ozone is reduced by ~ 2 ppmv (30%) inside the core of the anticyclone compared to regions near the anticyclone edge. Partial column ozone over the altitude range of the LOP (25–50 km) is shown in the right panel. Mean LOP partial column ozone is ~ 80 DU in the center of the anticyclone while partial column ozone in nearby ambient regions is ~ 120 DU. Thus the LOP effectively reduces the ozone column by ~ 40 DU over much of the Arctic western hemisphere on this day. This represents a reduction of $\sim 10\%$ in the total ozone column (estimated to be ~ 440 DU) due to the LOP. Typical amounts of ozone lost from the column due to LOPs are on the order of 10 to 25 DU or $\sim 3\text{--}6\%$. The example LOP shown here is representative in that it extends through a deep vertical layer. LOPs that extend to lower altitudes have a larger effect on the ozone column. Note, however, that the ozone lost from the column due to LOPs is typically mitigated by elevated ozone in the anticyclone below the LOP where the chemical lifetime of ozone is long compared to transport timescales. Thus while LOPs significantly affect ozone mixing ratios in the middle stratosphere, even large LOPs are not usually visible in total column ozone.

7. Conclusions

[26] MLS ozone data and MetO anticyclone information have been used to develop a new automated algorithm to

identify LOPs. This algorithm can be applied to other daily global ozone profile data such as from the High Resolution Dynamic Limb Sounder (HIRDLS) or from models for comparison to the MLS results. The MLS LOP observations span more than 3 years, from September 2004 to November 2007. LOP statistics compiled here include latitude, longitude, and altitude information, occurrence frequency and timing, and an estimate of the amount of ozone lost (both as a function of latitude, longitude, altitude and from the total ozone column).

[27] MLS results are qualitatively consistent with those based on SO data [Harvey et al., 2004] and show that most LOPs form in NH (SH) winter (spring). Zonal mean LOP statistics show that in the middle stratosphere near $50^\circ\text{--}70^\circ$ latitude in both hemispheres, MLS data points inside LOPs comprise over 15% of all ozone data points during these seasons. LOPs are identified poleward of $\sim 30^\circ$ latitude in both hemispheres and move poleward over their lifetimes, a direct consequence of the poleward migration of their parent anticyclones. However, nearly all LOP events occur in the persistent Aleutian and Australian anticyclones at middle and high latitudes. Ozone mixing ratios decline within individual LOPs as the LOPs move poleward, and LOPs deepen (have lower ozone) over the course of the winter. This is consistent with previous explanations that less solar insolation leads to less ozone production [Morris et al., 1998; Nair et al., 1998]. Deeper LOPs form in the NH compared to the SH due to the time of year in which they are most often observed (NH winter versus SH spring).

[28] Near the LOP frequency maxima from 28 to 36 km and $50^\circ\text{--}70^\circ$ latitude, zonal mean ozone during the LOP season is 10% (5%) lower in NH (SH) LOPs than in ambient air. Thus if the behavior in 2004–2007 is representative, LOPs cause an average seasonal zonal mean ozone loss from $50^\circ\text{--}70^\circ$ latitude of about 1.5% (0.75%) in the NH (SH). In both hemispheres, LOPs occur preferentially in the vicinity of the Date Line. Longitude-altitude sections show that, near 30 km, 50° latitude and the Date

Line, LOPs are identified on over 60% (50%) of NH winter (SH spring) days. This suggests that a LOP is present in the Aleutian and Australian anticyclones nearly all the time during these seasons. LOPs reduce ozone by up to 20% (10%) in the NH (SH) at these locations. The magnitude of these ozone differences agrees with monthly mean results of Harvey *et al.* [2004]. Thus seasonal estimates of the LOP contribution to midlatitude ozone variability in these regions are on the order of 12% in the NH and 5% in the SH. Daily ozone deficits averaged between 600 K and 1600 K (\sim 23–42 km) in LOPs range from 5–20%, but single profile differences at each altitude often exceed 50%. During the most extreme LOP event in January 2006, the ozone column was reduced by 10% for over 2 weeks; typically, LOPs reduce the ozone column by 3–6%. Future work will explore whether there are trends in LOP frequency by applying the automated algorithm to longer data records such as from the Solar Backscatter Ultraviolet (SBUV) and SBUV/2 instruments.

[29] **Acknowledgments.** We appreciate comments made by three anonymous reviewers that improved the quality of this manuscript. We would like to thank colleagues at the United Kingdom Meteorological Office for producing the MetO analyses. We thank the MLS instrument science team for the satellite data. We would also like to thank the Distributed Active Archive Center at the Goddard Space Flight Center and the British Atmospheric Data Centre for distributing the data. Work at the Jet Propulsion Laboratory, California Institute of Technology was done under contract with the National Aeronautics and Space Administration. This work was supported by NASA grants NNG06GI24G and NNG04GF39G.

References

- Abrams, M. C., et al. (1996), ATMOS/ATLAS-3 observations of long-lived tracers and descent in the Antarctic vortex in November 1994, *Geophys. Res. Lett.*, **23**, 2341–2344.
- Andersen, S. B., and B. M. Knudsen (2002), The influence of vortex ozone depletion on Arctic ozone trends, *Geophys. Res. Lett.*, **29**(21), 2013, doi:10.1029/2001GL014595.
- Chipperfield, P., and R. L. Jones (1999), Relative influences of atmospheric chemistry and transport on Arctic ozone trends, *Nature*, **400**, 551–554.
- Choi, W., S. Kim, W. B. Grant, M. Shiotani, Y. Sasano, and M. R. Schoeberl (2002), Transport of methane in the stratosphere associated with the breakdown of the Antarctic polar vortex, *J. Geophys. Res.*, **107**(D24), 8209, doi:10.1029/2001JD000644.
- Davies, T., et al. (2005), A new dynamical core for the met office's global and regional modeling of the atmosphere, *Q. J. R. Meteorol. Soc.*, **131**, 1759–1782.
- Froidevaux, L., et al. (2006), Early validation analyses of atmospheric profiles from EOS MLS on the Aura satellite, *IEEE Trans. Geosci. Remote Sens.*, **44**(5), 1106–1121.
- Froidevaux, L., et al. (2008), Validation of Aura Microwave Limb Sounder Stratospheric ozone measurements, *J. Geophys. Res.*, **113**, D15S20, doi:10.1029/2007JD008771.
- Fusco, A. C., and M. L. Salby (1999), Interannual variations of total ozone and their relationship to variations of planetary wave activity, *J. Clim.*, **12**, 1619–1629.
- Hadjinicolaou, P., A. Jrrar, J. A. Pyle, and L. Bishop (2002), The dynamically driven long-term trend in stratospheric ozone over northern mid-latitudes, *Q. J. R. Meteorol. Soc.*, **128**, 1393–1412.
- Harvey, V. L., and M. H. Hitchman (1996), A climatology of the Aleutian High, *J. Atmos. Sci.*, **53**, 2088–2101.
- Harvey, V. L., M. H. Hitchman, R. B. Pierce, and T. D. Fairlie (1999), Tropical aerosol in the Aleutian High, *J. Geophys. Res.*, **104**, 6281–6290.
- Harvey, V. L., R. B. Pierce, T. D. Fairlie, and M. H. Hitchman (2002), An object oriented climatology of stratospheric polar vortices and anticyclones, *J. Geophys. Res.*, **107**(D20), 4442, doi:10.1029/2001JD001471.
- Harvey, V. L., R. B. Pierce, M. H. Hitchman, C. E. Randall, and T. D. Fairlie (2004), On the distribution of ozone in stratospheric anticyclones, *J. Geophys. Res.*, **109**, D24308, doi:10.1029/2004JD004992.
- Hood, L. L., and B. Soukharev (2005), Interannual variations of total ozone at northern midlatitudes correlated with stratospheric EP flux and potential vorticity, *J. Atmos. Sci.*, **62**, 3724–25–3740.
- Hood, L. L., J. P. McCormack, and K. Labitzke (1997), An investigation of dynamical contributions to midlatitude ozone trends in winter, *J. Geophys. Res.*, **102**, 13,079–13,093.
- Hood, L. L., S. Rossi, and M. Belen (1999), Trends in lower stratospheric zonal winds, Rossby wave breaking behavior, and column ozone at northern midlatitudes, *J. Geophys. Res.*, **104**, 24,321–24,339.
- Hudson, R. D., A. D. Frolov, M. F. Andrade, and M. B. Follette (2003), The total ozone field separated into meteorological regimes. part I: Defining the regimes, *J. Atmos. Sci.*, **60**, 1669–1677.
- Hudson, R. D., M. F. Andrade, M. B. Follette, and A. D. Frolov (2006), The total ozone field separated into meteorological regimes. part II: Northern Hemisphere mid-latitude total ozone trends, *Atmos. Chem. Phys.*, **6**, 5183–5191.
- Kent, G. S., C. R. Trepte, U. O. Farrukh, and M. P. McCormick (1985), Variation in the stratospheric aerosol associated with the north cyclonic polar vortex as measured by the SAM II satellite sensor, *J. Atmos. Sci.*, **42**, 1536–1551.
- Kleinbohl, A., et al. (2005), Rapid meridional transport of tropical air-masses to the Arctic during the major stratospheric warming in January 2003, *Atmos. Chem. Phys.*, **6**, 1291–1299.
- Knudsen, B. M., and S. B. Andersen (2001), Longitudinal variation in springtime ozone trends, *Nature*, **413**, 699–700.
- Knudsen, B. M., W. A. Lanz, A. O'Neill, and J. J. Morcrette (1998), Evidence for a substantial role for dilution in northern mid-latitude ozone depletion, *Geophys. Res. Lett.*, **25**, 4501–4504.
- Kreher, K., G. E. Bodeker, H. Kanzawa, H. Nakane, and Y. Sasano (1999), Ozone and temperature profiles measured above Kiruna inside, at the edge of, and outside the Arctic polar vortex in February and March 1997, *Geophys. Res. Lett.*, **26**, 715–718.
- Lahoz, W. A., et al. (1993), Northern hemisphere mid-stratosphere vortex processes diagnosed from H₂O, N₂O and potential vorticity, *Geophys. Res. Lett.*, **20**, 2671–2674.
- Lahoz, W. A., et al. (1994), Three-dimensional evolution of water vapor distributions in the Northern Hemisphere stratosphere as observed by the MLS, *J. Atmos. Sci.*, **51**, 2914–2930.
- Lahoz, W. A., et al. (1996), Vortex dynamics and the evolution of water vapour in the stratosphere of the Southern Hemisphere, *Q. J. R. Meteorol. Soc.*, **122**, 423–450.
- Livesey, N. J., et al. (2008), Validation of Aura Microwave Limb Sounder O₃ and CO observations in the upper troposphere and lower stratosphere, *J. Geophys. Res.*, **113**, D15S02, doi:10.1029/2007JD008805.
- Lorenc, A. C., et al. (2000), The Met. Office global three-dimensional variational data assimilation scheme, *Q. J. R. Meteorol. Soc.*, **126**, 2991–3012.
- Manney, G. L., J. D. Farrara, and C. R. Mechoso (1991), The behavior of wave 2 in the southern hemisphere stratosphere during late winter and early spring, *J. Atmos. Sci.*, **48**, 976–998.
- Manney, G. L., et al. (1994), Stratospheric warmings during February and March 1993, *Geophys. Res. Lett.*, **21**, 813–816.
- Manney, G. L., et al. (1995), Formation of low-ozone pockets in the middle stratospheric anticyclone during winter, *J. Geophys. Res.*, **100**, 13,939–13,950.
- Manney, G. L., et al. (1999), Polar vortex dynamics during spring and fall diagnosed using trace gas observations from the Atmospheric Trace Molecule Spectroscopy instrument, *J. Geophys. Res.*, **104**, 18,841–18,866.
- Manney, G. L., et al. (2006), EOS Microwave Limb Sounder observations of “frozen-in” anticyclonic air in Arctic summer, *Geophys. Res. Lett.*, **33**, L06810, doi:10.1029/2005GL025418.
- Manney, G. L., et al. (2008a), The evolution of the stratopause during the 2006 major warming: Satellite data and assimilated meteorological analyses, *J. Geophys. Res.*, **113**, D11115, doi:10.1029/2007JD009097.
- Manney, G. L., et al. (2008b), The high Arctic in extreme winters: Vortex, temperature, and MLS and ACE-FTS trace gas evolution, *Atmos. Chem. Phys.*, **8**, 505–522.
- Mechoso, C. R., A. O'Neill, V. D. Pope, and J. D. Farrara (1988), A study of the stratospheric final warming of 1982 in the Southern Hemisphere, *Q. J. R. Meteorol. Soc.*, **114**, 1365–1384.
- Morris, G. A., S. R. Kawa, A. R. Douglass, and M. R. Schoeberl (1998), Low ozone pockets explained, *J. Geophys. Res.*, **103**, 3599–3610.
- Nair, H., M. Allen, L. Froidevaux, and R. W. Zurek (1998), Localized rapid ozone loss in the northern winter stratosphere: An analysis of UARS observations, *J. Geophys. Res.*, **103**, 1555–1571.
- O'Neill, A., W. Grose, V. D. Pope, H. Maclean, and R. Swinbank (1994), Evolution of the stratosphere during Northern winter 1991/92 as diag-

- nosed from U. K. Meteorological Office analyses, *J. Atmos. Sci.*, **51**, 2800–2817.
- Randall, C. E., et al. (1995), Preliminary results from POAM II: Stratospheric ozone at high northern latitudes, *Geophys. Res. Lett.*, **22**, 2733–2736.
- Randall, C. E., et al. (1996), An overview of POAM II aerosol measurements at 1.06 μm , *Geophys. Res. Lett.*, **23**, 3195–3198.
- Randel, W. J., F. Wu, and R. Stolarski (2002), Changes in column ozone correlated with stratospheric EP flux, *J. Meteorol. Soc. Jpn.*, **80**, 849–862.
- Schoeberl, M. R., L. R. Lait, P. A. Newman, and J. E. Rosenfield (1992), The structure of the polar vortex, *J. Geophys. Res.*, **97**, 7859–7882.
- Scott, R. K., and D. G. Dritschel (2006), Vortex-Vortex interactions in the winter stratosphere, *J. Atmos. Sci.*, **63**, 726–740.
- Sutton, R. T., H. Maclean, R. Swinbank, A. O'Neill, and F. W. Taylor (1994), High-resolution stratospheric tracer fields estimated from satellite observations using Lagrangian trajectory calculations, *J. Atmos. Sci.*, **51**, 2995–3005.
- Swinbank, R., and A. O'Neill (1994), A stratosphere-troposphere data assimilation system, *Mon. Weather Rev.*, **122**, 686–702.
- Waters, J. W., et al. (2006), The Earth Observing System Microwave Limb Sounder (EOS MLS) on the Aura satellite, *IEEE Trans. Geosci. Remote Sens.*, **44**, 1075–1092.

V. L. Harvey and C. E. Randall, Laboratory for Atmospheric and Space Physics, University of Colorado, Boulder, CO 80309-0392, USA.
(lynn.harvey@lasp.colorado.edu)

G. L. Manney, Jet Propulsion Laboratory, California Institute of Technology, Mail Stop 183-701, Pasadena, CA 91109, USA.

C. S. Singleton, National Science Foundation, 4201 Wilson Boulevard, Arlington, VA 22230, USA.